A Spin Topological Model for the $g = 4.1$ S_2 State Photosystem II Water Oxidase Manganese Aggregate

Christopher E. Dubé,*[,†,‡] Roberta Sessoli,[§] Michael P. Hendrich,[⊥] Dante Gatteschi,[§] and William H. Armstrong*[,†]

Departments of Chemistry
Eugene F. Merkert Chemistry Center, Boston College
Chestnut Hill, Massachusetts 02167-3860
University of Florence
Florence, Italy 50144
Carnegie Mellon University
Pittsburgh, Pennsylvania 15213

Received November 30, 1998

The oxygen-evolving complex (OEC) of photosystem II (PSII) catalyzes photosynthetic oxidation of water to molecular oxygen. Although the precise structure of the OEC is unknown, spectroscopic and magnetic studies suggest that it contains a high-valence, magnetically coupled tetranuclear manganese−oxo aggregate.[1−3] X-band electron paramagnetic resonance (EPR) spectroscopy of the S_2 oxidation state reveals three characteristic signals associated with the manganese aggregate: a 19−21 line signal centered at $g = 2$,[4] signals at $g > 5$,[5] and a signal centered at $g = 4.1$.[6,7] Conversion of the $g = 4.1$ form to the S_2 multiline signal upon annealing at 195 K[6,7] and conversion of the multiline form to the $g = 4.1$ form with near-IR irradiation[5,8] substantiated the proposal[9] that both signals came from the same cluster. The $g = 4.1$ signal has been attributed to either an axial $S = 3/2$ [9−12] or near-rhombic ($E/D \sim 1/3$) $S = 5/2$ multiplet.[13−15] Recent analysis of the low-temperature magnetization of the OEC of PSII is consistent with an $S = 5/2$ state with $D = 1.7$ (or -1.05) cm^{-1} and $E/D = 0.25$.[16] Here we report the magnetic behavior and EPR analysis of the first tetranuclear, high-valence manganese−oxo aggregate with an $S = 5/2$ ground state, $[Mn_4O_6(bpea)_4]^{3+}$ (**1**).[17,18] This pseudo-tetrahedral arrangement of $Mn^{III}(Mn^{IV})_3$ ions is proposed as a spin topological model for the $g = 4.1$ S_2 state of the PSII water oxidase manganese cluster.

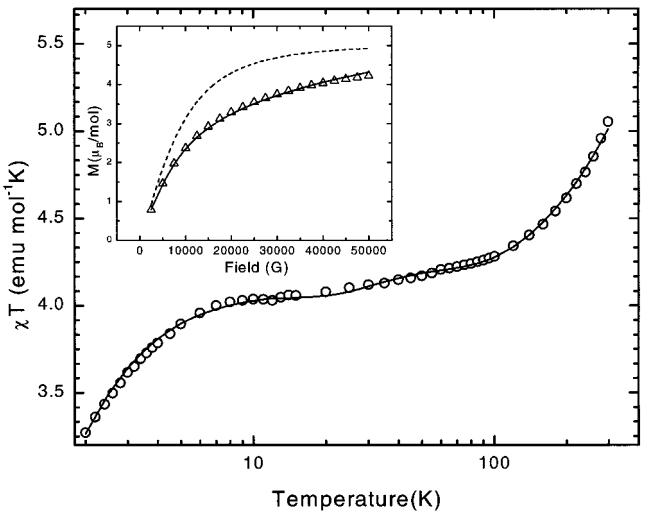

Figure 1. Temperature dependence of the χT product of **1**$(BAr'_4)_3$ measured at 0.5 T (○) showing the best fit (—) of the theoretical expression. Inset: Isothermal magnetization of **1**$(BAr'_4)_3$ at 2.00 K (△) and best fit (—) of the $S = 5/2$ state. The dashed line corresponds to the Brillouin function expected for an isolated $S = 5/2$ state with no zero-field splitting.

Previously, we showed by solution magnetic susceptibility measurements[19] at 295 K that one-electron reduction of $[Mn_4O_6(bpea)_4](ClO_4)_4$ (**2**$(ClO_4)_4$) ($\chi T = 10.9$ emu mol^{-1} K) to **1**$(ClO_4)_3$ ($\chi T = 5.09$ emu mol^{-1} K) is attendant with a change from ferromagnetic coupling to overall moderate antiferromagnetic coupling within the manganese−oxo core.[18] Analysis of the magnetic susceptibility measurements on a powdered sample of **2**$(ClO_4)_4$ with a two-J Heisenberg exchange Hamiltonian confirms ferromagnetic interactions within **2**.[20]

The χT product/tetramer versus temperature for mixed-valence **1**$(BAr'_4)_3$[18] is shown in Figure 1. The value of χT for **1**$(BAr'_4)_3$ at 295 K (5.03 emu mol^{-1} K) is in good agreement with the solution value of **1**$(ClO_4)_3$. Qualitative analysis suggests that the ground spin state of the cluster is $S = 5/2$ with a sizable zero-field splitting, in agreement with the presence of a Jahn−Teller distorted Mn^{III} ion (S_3 in Figure 2). The χT data were quantitatively analyzed assuming isotropic Heisenberg interactions and including a zero-field splitting term as a perturbation in the ground state only. The $\{Mn_4O_6\}$ core structure of **1**[18] reveals that there are five types of bridging oxo ligands in **1**, leading to five exchange coupling constants (Figure 2).

Figure 1 shows a plot of the fit of the theoretical expression to the experimental data, with the best-fit parameters $g = 1.93$, $J_{12} = J_{24} = J_{A'} = 8.5$ cm^{-1}, $J_{14} = J_{B'} = 73$ cm^{-1}, $J_{13} = J_{JT} = 33$ cm^{-1}, $J_{23} = -190$ cm^{-1}, $J_{34} = -12$ cm^{-1}, $D = 1.1$ cm^{-1}, and $E/D = 0.20$.[21] The ferromagnetic exchange between the Mn^{IV} ions of **1** ($J_{A'} = 8.5$ cm^{-1} and $J_{B'} = 73$ cm^{-1} for types A and B oxo bridges, respectively) is close to that found for geometrically

[†] Boston College.
[§] University of Florence.
[⊥] Carnegie Mellon University.
[‡] Present address: Symyx Technologies, Santa Clara, CA 95051.

(1) Britt, R. D. In *Oxygenic Photosynthesis: The Light Reactions*; Ort, D. R., Yocum, C. F., Eds.; Kluwer Academic Publishers: Dordrecht, The Netherlands, 1996; pp 137−164.
(2) Yachandra, V. K.; Sauer, K.; Klein, M. P. *Chem. Rev.* **1996**, *96*, 2927−2950.
(3) Penner-Hahn, J. E. In *Structure and Bonding*; Hill, H. A. O., Sadler, P. J., Thomson, A. J., Eds.; Springer-Verlag: Berlin, 1998; Vol. 90, pp 1−36.
(4) Dismukes, G. C.; Siderer, Y. *FEBS Lett.* **1980**, *121*, 78−80.
(5) Boussac, A.; Un, S.; Horner, O.; Rutherford, A. W. *Biochemistry* **1998**, *37*, 4001−4007.
(6) Casey, J. L.; Sauer, K. *Biochim. Biophys. Acta* **1984**, *767*, 21−28.
(7) Zimmermann, J. L.; Rutherford, A. W. *Biochim. Biophys. Acta* **1984**, *767*, 160−167.
(8) Boussac, A.; Girerd, J.-J.; Rutherford, A. W. *Biochemistry* **1996**, *35*, 6984−6989.
(9) de Paula, J. C.; Beck, W. F.; Brudvig, G. W. *J. Am. Chem. Soc.* **1986**, *108*, 4002−4009.
(10) Hansson, Ö.; Aasa, R.; Vänngård, T. *Biophys. J.* **1987**, *51*, 825−832.
(11) Smith, P. J.; Åhrling, K. A.; Pace, R. J. *J. Chem. Soc., Faraday Trans.* **1993**, *89*, 2863−2868.
(12) Åhrling, K. A.; Smith, P. J.; Pace, R. J. *J. Am. Chem. Soc.* **1998**, *120*, 13202−13214.
(13) Vänngård, T.; Hansson, Ö.; Haddy, A. In *Manganese Redox Enzymes*; Pecoraro, V. L., Ed.; VCH Publishers: New York, 1992; pp 105−118.
(14) Haddy, A.; Dunham, W. R.; Sands, R. H.; Aasa, R. *Biochim. Biophys. Acta* **1992**, *1099*, 25−34.
(15) Astashkin, A. V.; Kodera, Y.; Kawamori, A. *J. Magn. Reson.* **1994**, *105B*, 113−119.
(16) Horner, O.; Rivière, E.; Blondin, G.; Un, S.; Rutherford, A. W.; Girerd, J.-J.; Boussac, A. *J. Am. Chem. Soc.* **1998**, *120*, 7924−7928.
(17) Abbreviations Used: bpea, *N*,*N*-bis(2-pyridylmethyl)ethylamine; BAr'_4^-, $[[3,5\text{-}(CF_3)_2C_6H_3]_4B]^-$.
(18) Dubé, C. E.; Wright, D. W.; Pal, S.; Bonitatebus, P. J., Jr.; Armstrong, W. H. *J. Am. Chem. Soc.* **1998**, *120*, 3704−3716.
(19) Evans, D. J. *J. Chem. Soc.* **1959**, 2003−2005.
(20) Magnetic data were analyzed by using the Hamiltonian in the form $H = -(J_{12}\mathbf{S_1S_2} + J_{13}\mathbf{S_1S_3} + J_{14}\mathbf{S_1S_4} + J_{23}\mathbf{S_2S_3} + J_{24}\mathbf{S_2S_4} + J_{34}\mathbf{S_3S_4})$. The two types of oxo bridges within the cluster (Types A and B) give rise to two different exchange interactions, with $J_{12} = J_{13} = J_{24} = J_{34} = J_A = 10.2$ cm^{-1} and $J_{14} = J_{23} = J_B = 90.0$ cm^{-1}, and $g = 1.88$ (R. Sessoli et al., manuscript in preparation).
(21) The value of $E/D = 0.20$ was based on analysis of the EPR spectrum of **1**$(ClO_4)_3$. The large number of parameters is required by the structural and spin topological features of the cluster. Attempts to use fewer parameters gave a lower quality fit of the data.

10.1021/ja9840910 CCC: $18.00
Published on Web 03/24/1999

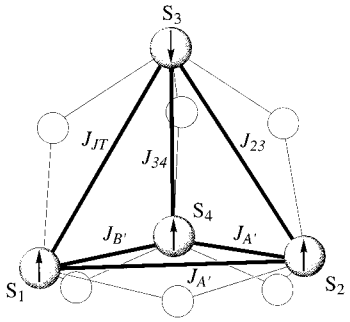

Figure 2. Spin topology and assignment of exchange coupling constants for Mn−Mn interactions of **1**. The spin label S_3 designates the Mn^{III} ion, and S_1, S_2, and S_4 designate the Mn^{IV} ions, with corresponding atom labels Mn(3), Mn(1), Mn(2), and Mn(4), respectively.

similar[18] oxo ligand bridges in **2** (J_A= 10.2 cm^{-1} and J_B = 90.0 cm^{-1}, for type A and B, respectively). Antiferromagnetic interactions observed for the Mn(2)−Mn(3) and Mn(3)−Mn(4) pairs are mediated through oxygen atoms in equatorial coordination to Mn(3). A ferromagnetic interaction between Mn(1)−Mn(3) is consistent with axial coordination of oxygen to Mn(3).[22,23] Rapid decrease of χT below 10 K can be attributed to the presence of zero-field splitting. The $S = 5/2$ ground state of **1** and the zero-field splitting have been confirmed by the field dependence of the magnetization measured at 2.00 K (Figure 1, inset). The field dependence of the magnetization has been adequately fit as an $S = 5/2$ ion with an E/D ratio of 0.20 and D = 1.1 cm^{-1}.[24] We estimate that $|D(S = 5/2)| = 1.1$ cm^{-1} corresponds to $|D(Mn^{III})| = 5.1$ cm^{-1},[25] which compares well with values obtained for other Mn^{III} compounds.[26]

The EPR spectrum of $\mathbf{1}(ClO_4)_3$ (Figure 3) is dominated by a broad signal centered at about 1600 G ($g \sim 4.1$), with a low field component of $g \sim 9.1$.[27] The simulation of the EPR signal of **1** (Figure 3) indicates a ground spin manifold of $S = 5/2$ with $E/D = 0.20$. The signals at $g = 9.1$ and 4.1 are from the lowest and first excited Kramers doublets, respectively. The simulation was calculated with diagonalization of the spin Hamiltonian, $H = D(S_z^2 - S(S + 1)/3) + E(S_x^2 - S_y^2) + \beta B \cdot g \cdot S$, and polycrystalline summation over a uniform spherical angular array. The line shape is accurately modeled with a Gaussian distribution in E/D of width $\sigma_{E/D} = 0.086$ and a homogeneous spin-packet line width of σ_B = 15 mT.[28]

The spin value of the $g = 4.1$ signal for the S_2 state of the OEC is the subject of much interest and is proposed to be either from an S = 3/2[9−12] or $S = 5/2$ state.[13−16] Figure 3 (inset) illustrates the strong resemblance between the low-temperature X-band spectrum of **1** and the $g = 4.1$ OEC signal.[29] In addition, the D value determined here for **1** (1.1 cm^{-1}) is close to that estimated for the OEC (1.7 cm^{-1}).[16] The $\{Mn_4O_6\}^{3+}$ core of **1,** described here as a $Mn^{III}(Mn^{IV})_3$ pseudotetrahedron, also exhibits oxidation state parity with our preferred assignment of the S_2 state.[2,30] Thus, we demonstrate experimentally for the first time here using the synthetic complex **1** that the $g = 4.1$ S_2 state of PSII may arise from the spin topology shown in Figure 2: a pseudotetrahedral array of Mn ions with three ferromagnetically coupled Mn(IV) ions and a Mn(III) ion with opposing spin alignment.[31]

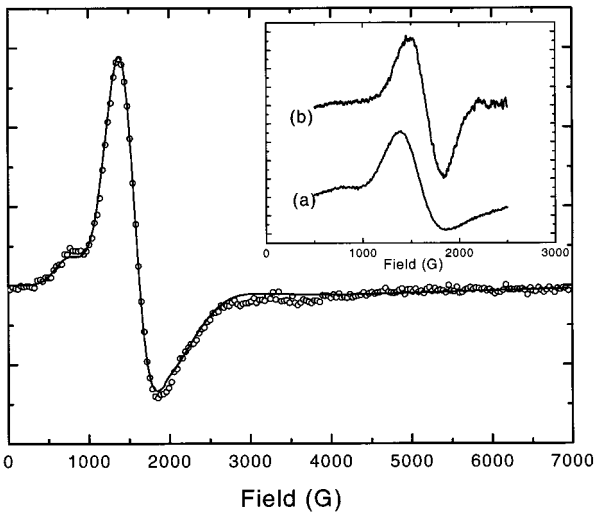

Figure 3. X-band EPR spectrum of an acetonitrile solution of $\mathbf{1}(ClO_4)_3$ measured at 30 K (○) and least-squares simulation (—). Inset: Comparison of the X-band EPR spectra of (a) $\mathbf{1}(ClO_4)_3$ and (b) PSII enriched membranes (9.484 GHz, 11.5 mg Chl/mg in buffer, 10 K). Sample was illuminated for 6 min at 195 K.[29] Microwave power and modulation amplitude: 2 mW and 3.2 G, and 20 mW and 16 G, for $\mathbf{1}(ClO_4)_3$ and PSII samples, respectively.

Acknowledgment. We thank Prof. H. Weihe for a copy of the EPR simulation program used in some of our EPR simulations and Prof. A. Haddy for use of her EPR spectrum of the $g = 4.1$ S_2 state of the PSII OEC. W.H.A. and C.E.D. acknowledge funding by National Institutes of Health grant GM38275. The W. M. Keck Foundation provided funds for the SQUID magnetometer at Tufts University. D.G. and R.S. acknowledge financial support of Ministero dell' Universitá e della Ricerca Scientifica e Tecnologica.

JA9840910

(22) Hotzelmann, R.; Wieghardt, K.; Florke, U.; Haupt, H.; Weatherburn, D. C.; Bonvoisin, J.; Blondin, G.; Girerd, J. *J. Am. Chem. Soc.* **1992**, *114*, 1681−1696.

(23) Kahn, O. In *Magneto-Structural Correlations in Exchange Coupled Systems*; Willett, R. D. G., D.; Kahn, O., Eds.; D. Reidel: Dordrecht, 1985; pp 37−56.

(24) In this analysis we assume that the contribution given by the single ion zero-field splitting (zfs) of the Mn^{III} site dominates and we neglect the contributions from single ion Mn^{IV} zfs, as well as those introduced by anisotropic interactions.

(25) Bencini, A.; Gatteschi, D. In *EPR of Exchange Coupled Systems*; Springer-Verlag: Berlin, 1990; pp 86−120.

(26) Barra, A.-L.; Gatteschi, D.; Sessoli, R.; Abbati, G. L.; Cornia, A.; Fabretti, A. C.; Uytterhoeven, M. G. *Angew. Chem., Int. Ed. Engl.* **1997**, *36*, 2329−2331.

(27) Low-temperature (3.5−77 K) X-band (9.41 GHz) EPR measurements were performed on a 10.2 mM acetonitrile solution of $\mathbf{1}(ClO_4)_3$. The EPR spectrum of $\mathbf{1}(ClO_4)_3$ was corrected for a trace amount of $\mathbf{2}(ClO_4)_4$ impurity by subtraction of the EPR spectrum of $\mathbf{2}(ClO_4)_4$.

(28) Both distribution parameters are required to match the simulation to the data. The large value of $\sigma_{E/D}$ reflects small structural variations. The large value of σ_B is likely the result of unresolved ^{55}Mn hyperfine splitting. Samples of various concentrations did not show resolved hyperfine, suggesting that the broad lines are not due to molecule aggregation. Additional details concerning the simulation program will be in a forthcoming publication.

(29) A. Haddy, private communication.

(30) Bergmann, U.; Grush, M. M.; Horne, C. R.; DeMarios, P.; Penner-Hahn, J. E.; Yocum, C. F.; Wright, D. W.; Dubé, C. E.; Armstrong, W. H.; Christou, G.; Eppley, H. J.; Cramer, S. P. *J. Phys. Chem. B* **1998**, *102*, 8350−8352.

(31) While the adamantane-shaped core of **1** is a spin coupling/spin topological model for the $g = 4.1$ S_2 state, we note that EXAFS studies of the Mn−oxo core within PSII reveal at least two 2.7 Å Mn···Mn vectors, thus compound **1** cannot be considered an accurate geometrical model for the S_2 state manganese aggregate.